

FD Simulation for Long-Period Ground Motions of Great Nankai Trough, Japan, Earthquakes



T. Maeda, N. Morikawa, S. Aoi, & H. Fujiwara

National Research Institute for Earth Science and Disaster Prevention, Japan

SUMMARY:

Long-period ground motions of the anticipated Nankai Trough earthquake in southwest Japan (recurrence time of 100 to 200 years) were simulated by the finite difference method using the characterized source model and recently developed three-dimensional velocity structure model of Japan. To understand a possible range of long-period ground motion caused by the uncertainty of source model, we simulated long-period ground motions using 55 scenarios with various possible parameters including rupture area, asperity location, and hypocenter. The simulation results showed the large variation depending on different scenarios. This large variation can help us to understand a possible range of long-period ground motions from the anticipated Nankai Trough earthquake.

Keywords: Nankai Trough earthquake, long-period ground motion, finite difference method, GMS, uncertainty

1. INTRODUCTION

Megathrust earthquakes in the Nankai Trough in southwest Japan have been occurring with an interval of 100-200 years. Mainly, there are two patterns of Nankai Trough earthquake. One is the series of smaller earthquakes in short time period and second is the single larger event ruptured at once. The most recent example of the first case is the series of earthquake in 1944 Tonankai earthquake (M7.9) and in 1946 Nankai earthquake (M8.0). The most recent example of the second case is the 1707 Hiei earthquake (M8.4).

For improving seismic hazard assessment to prepare for the anticipated Nankai Trough earthquake, it is important to understand a possible range of ground motion caused by uncertainty of source model. In this study, we evaluate long-period ground motions of the Nankai Trough earthquake, which will cause damage to high-rise and large-scale structures, using many scenarios with various possible parameters including rupture area, asperity location, and hypocenter. In the possible parameters, we also include the scenario; the large slip near the trough following the lesson from the 2011 Tohoku earthquake. The long-period ground motions are simulated by the finite difference method using characterized source model and recently developed three-dimensional velocity structure model of Japan.

2. CHARACTERIZED SOURCE MODEL

We use the characterized source model in the long-period ground motion simulation. At first we define source areas of the Nankai Trough earthquakes. An occurrence pattern of the Nankai Trough earthquakes is assumed that the respective earthquakes occur independently or that multiple earthquakes occur in a correlated manner. Thus we model source areas for the respective earthquakes (Fig. 2.1). The source areas of the Nankai earthquake (ANNKI), the Tonankai earthquake (ATNKI), and the hypothetical Tokai earthquake (ATOKI) are based on the model reported by Earthquake

Table 2.1 Source Parameters Used In The FD Simulation

		ANNKI	ATNKI	ATOKI	ATRGH	AHGND	ANNI1	ANNI2	ANNI3	ANNI4	ANNI5		
total	S (km ²)	35800	14500	9400	12500	19000	51200	23600	60300	72800	80500		
	M ₀ (Nm)	8.3.E+21	2.2.E+21	1.1.E+21	1.7.E+21	3.2.E+21	1.4.E+22	4.5.E+21	1.8.E+22	2.4.E+22	2.8.E+22		
	Δσ (MPa)	3.0	3.0	3.0	3.0	3.0	3.0	3.0	3.0	3.0	3.0		
	M _w	8.5	8.2	8.0	8.1	8.3	8.7	8.4	8.8	8.9	8.9		
asperity	Nankai	1	S (km ²)	3580	-	-	-	-	3580	-	3580	3580	3580
			M _{0a} (Nm)	2.1.E+21	-	-	-	-	2.9.E+21	-	3.3.E+21	3.6.E+21	4.0.E+21
			Δσ _a (MPa)	15.0	-	-	-	-	15.3	-	15.2	15.1	15.3
		2,3	S (km ²)	1790	-	-	-	-	1790	-	1790	1790	1790
			M _{0a} (Nm)	7.6.E+20	-	-	-	-	1.0.E+21	-	1.2.E+21	1.3.E+21	1.4.E+21
			Δσ _a (MPa)	15.0	-	-	-	-	15.3	-	15.2	15.1	15.3
	Tonankai	1	S (km ²)	-	1450	-	-	-	1450	1450	1450	1450	1450
			M _{0a} (Nm)	-	5.5.E+20	-	-	-	7.4.E+20	7.7.E+20	8.6.E+20	9.2.E+20	1.0.E+21
			Δσ _a (MPa)	-	15.0	-	-	-	15.3	14.8	15.2	15.1	15.3
		2,3	S (km ²)	-	725	-	-	-	725	725	725	725	725
			M _{0a} (Nm)	-	2.0.E+20	-	-	-	2.6.E+20	2.7.E+20	3.0.E+20	3.2.E+20	3.6.E+20
			Δσ _a (MPa)	-	15.0	-	-	-	15.3	14.8	15.2	15.1	15.3
	Tokai	1	S (km ²)	-	-	940	-	-	-	940	940	940	940
			M _{0a} (Nm)	-	-	2.9.E+20	-	-	-	4.0.E+20	4.5.E+20	4.8.E+20	5.4.E+20
			Δσ _a (MPa)	-	-	15.0	-	-	-	14.8	15.2	15.1	15.3
		2,3	S (km ²)	-	-	470	-	-	-	470	470	470	470
			M _{0a} (Nm)	-	-	1.0.E+20	-	-	-	1.4.E+20	1.6.E+20	1.7.E+20	1.0.E+01
			Δσ _a (MPa)	-	-	15.0	-	-	-	14.8	15.2	15.1	15.3
	along trough	a,	S (km ²)	-	-	-	2500	-	-	-	-	2500	-
		b,	M _{0a} (Nm)	-	-	-	7.6.E+20	-	-	-	-	2.1.E+21	-
		c	Δσ _a (MPa)	-	-	-	15.0	-	-	-	-	15.1	-
	Hyuganada	1	S (km ²)	-	-	-	-	1900	-	-	-	-	1900
			M _{0a} (Nm)	-	-	-	-	8.3.E+20	-	-	-	-	1.5.E+21
			Δσ _a (MPa)	-	-	-	-	15.0	-	-	-	-	15.3
2,3		S (km ²)	-	-	-	-	950	-	-	-	-	950	
		M _{0a} (Nm)	-	-	-	-	2.9.E+20	-	-	-	-	5.4.E+20	
		Δσ _a (MPa)	-	-	-	-	15.0	-	-	-	-	15.3	
back ground	S (km ²)	28640	11600	7520	10000	15200	41140	18820	48360	58360	64760		
	M _{0b} (Nm)	4.7.E+21	1.2.E+21	6.3.E+20	9.6.E+20	1.8.E+21	8.1.E+21	2.5.E+21	1.0.E+22	1.4.E+22	1.6.E+22		
	Δσ _b (MPa)	1.8	1.8	1.8	3.0	1.8	1.4	1.3	1.2	1.1	1.0		

Research Committee (2001). We also model the source area of Hyuga-nada (AHGND), since Furumura et al. (2011) pointed out that a source area of the 1707 Hoei earthquake extends to the Hyuga-nada. In addition, we assume the large slip area along the trough following the lesson from the 2011 Tohoku earthquake and model three source areas along the trough (Fig. 2.1; ATRGHa-c). We model source areas for the case of correlated occurrence as a combination of the respective source area. These are the Nankai-Tonankai area (ANNI1), the Tonankai-hypothetical Tokai area (ANNI2), the Nankai-Tonankai-hypothetical Tokai area (ANNI3), the Nankai-Tonankai-hypothetical Tokai area with along the trough area (ANNI4a-c), and the Nankai-Tonankai-hypothetical Tokai area with the Hyuga-nada area (ANNI5).

The characterized source model is defined by three kinds of parameters: outer, inner, and extra fault parameters. The parameters are determined based on a ‘recipe’ for predicting strong ground motion (Irikura and Miyake, 2001). The outer fault parameters define an overall character of the source model. We estimate the rupture area S for each source area by taking into account geometry of plate interface and then calculate seismic moment M_0 and average slip D by assuming an average stress drop $\Delta\sigma_c$ of 3.0 MPa and rigidity of 40.4 GPa.

As for the inner fault parameters, combined area of asperities (a large slip areas) S_a and average slip

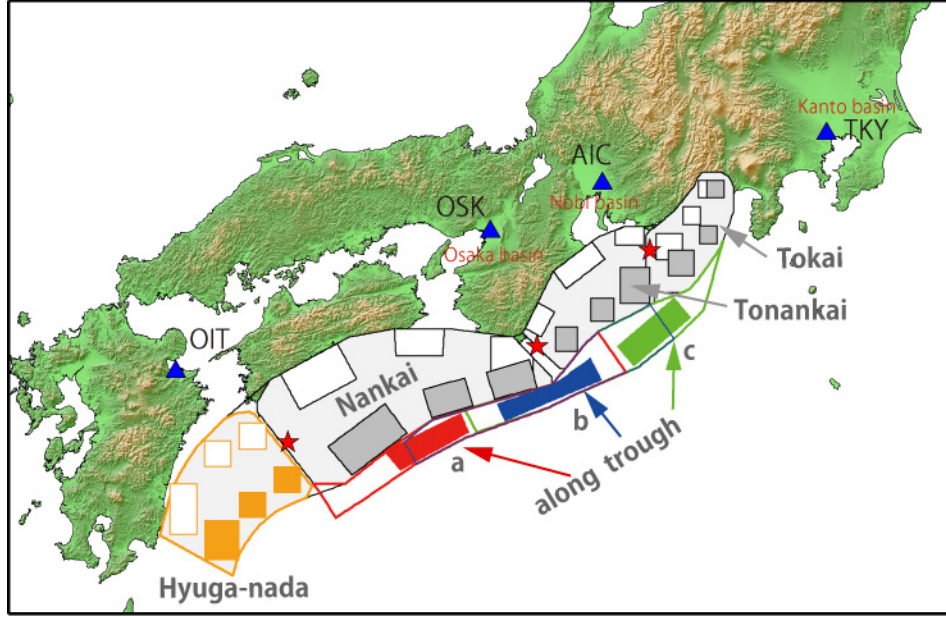


Figure 2.1. Characterized source models for the Nankai Trough earthquakes. Grey regions are the source area of the Nankai, Tonankai, and hypothetical Tokai earthquakes. Orange region is a source area of Hyuga-nada. Red, blue and green regions are source areas along the trough. Solid and open squares in the source area are asperities of shallower and deeper cases, respectively. Red stars are the hypocenters. Blue triangles are the sites for comparing simulation results.

of asperities D_a are derived by a scaling relationship to the seismic moment proposed by Murotani et al. (2008); $S_a = 0.2S$ and $D_a = 2.2D$. The number of asperity for the ANNKI, ATNKI, ATOKI, and AHGND is three and their area ratio is 2:1:1, while the number of asperity for ATRGHa-c is one. We assume two kinds of asperity location; deeper and shallower cases. The average slip of each asperity D_{ai} is derived by $D_{ai} = (\gamma_i / \sum \gamma_j^3) D_a$, where $\gamma_i = \sqrt{S_{ai} / S_a}$. The stress drop on asperities $\Delta\sigma_a$ is derived by $\Delta\sigma_a = \Delta\sigma_c (S / S_a)$. The stress drop on background σ_b is derived by $\sigma_b = (D_b / W_b) \cdot (\sqrt{\pi} / D_a) \cdot r \cdot \sum \gamma_i^3 \cdot \sigma_a$, where r is a radius of asperity and W_b is a fault width (we assume $W_b = \sqrt{S/2}$). As for the case of correlated occurrence, we assume that the asperity area is similar to the respective earthquake and calculate average slip and seismic moment with respect to a total rupture area. Source parameters are shown in Table 2.1. We use a slip velocity time function approximated from dynamic rupture simulation proposed by Nakamura and Miyatake (2000).

The extra fault parameters define a propagation pattern of rupture. We assume three hypocenters; west (boundary of Nankai and Hyuga-nada areas), center (boundary of Nankai and Tonankai areas), and east (boundary of Tonankai and Tokai areas). The rupture propagates radially from the hypocenter at a constant rupture velocity (2.7km/s). The rupture in each asperity starts from a point at the moment the rupture front reaches the point.

3. LONG-PERIOD GROUND MOTION SIMULATION

We simulate long-period ground motions using a three dimensional (3-D) finite difference (FD) simulation with discontinuous grids (Aoi and Fujiwara, 1999; Aoi et al., 2004). To accommodate details of 3-D subsurface structures into the FD model, we use discontinuous grids that consist of a fine grid spacing of 200 m in horizontal and of 100m in vertical for regions shallower than 8 km that contain low-velocity sedimentary layers, and a three times coarser grid spacing for deeper regions (8 ~ 70 km). The total number of grid points is about 20 billion. The 3-D velocity structure model used in the FD simulation is the Japan integrated velocity structure model (Koketsu et al., 2008), which includes basin, crust, plate and oceanic structures. The lowest S-wave velocity is 500m/s in the

structure model and thus the FD simulation is valid for period more than 2 second. However the characterized source model used in the FD simulation does not contain short period component, and thus we consider that the FD simulation is valid for period more than about 5 second. Inelastic attenuation is introduced in the same way as in Graves (1996) and we assume a reference period for Q -value of 5 second.

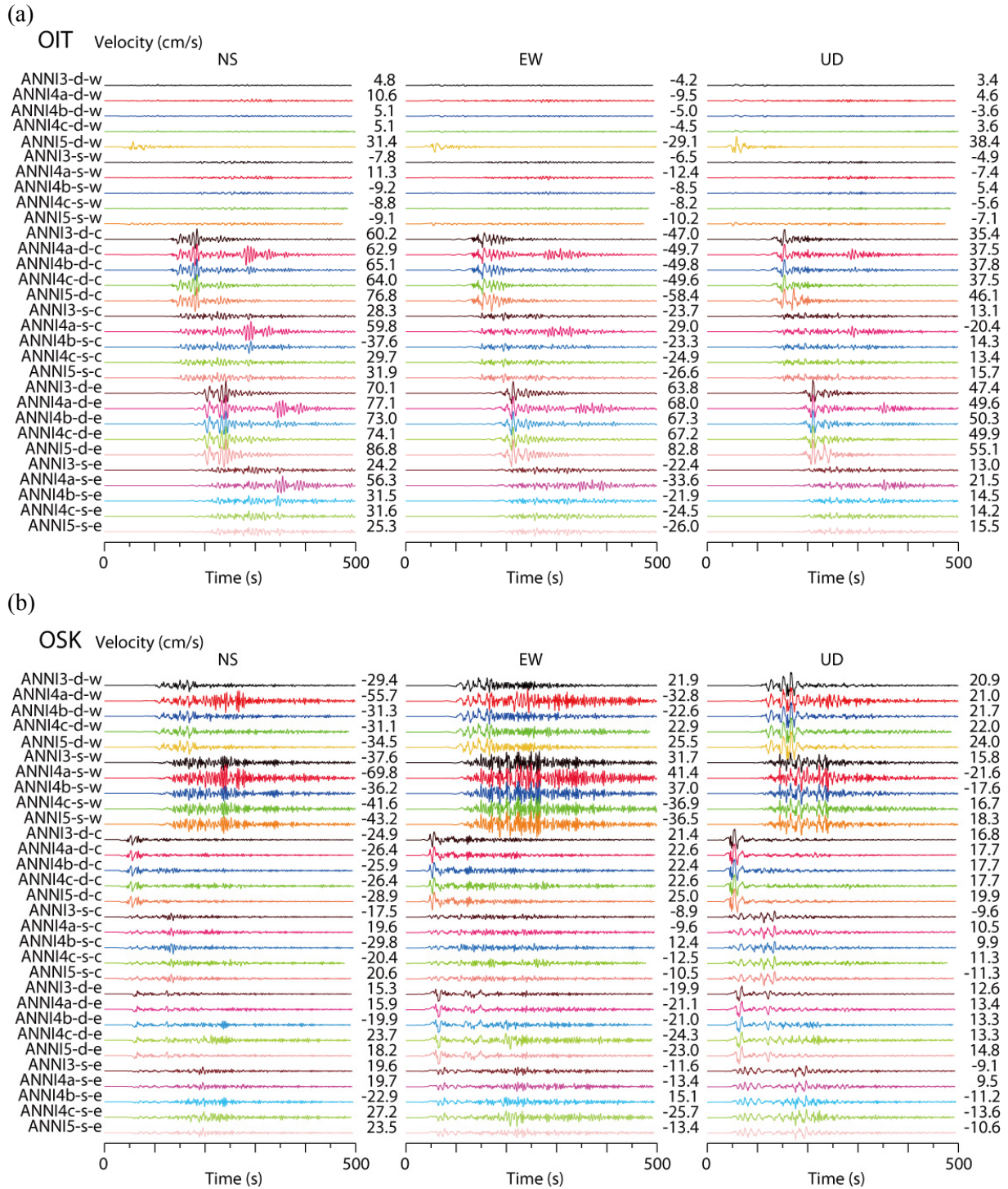


Figure 4.1. Results of the 3-D FD simulation for 30 scenarios at (a) OIT, (b) OSK, (c) AIC, and (d) TKY. Scenario name shown in the left means [source area]-[asperity location (deep, shallow)]-[hypocenter (west, center, east)]. The numbers on the right indicate the peak amplitude.

4. RESULTS

We simulate long-period ground motions for 55 scenarios. Figure 4.1 compares the simulated ground velocity for scenarios ANNI3, ANNI4a-c, and ANNI5 with different hypocenter and asperity location at Oita (OIT), Osaka (OSK), Nagoya in Aichi (AIC), and Shinjuku in Tokyo (TKY). In general, the hypocenter has a greater impact on waveforms, followed by the asperity location, and then the rupture area. S waves from deeper asperities of the Nankai area and later phases from the along trough 'a' area have significant influence at OIT and OSK. Later phases from the along trough 'c' area dominate at

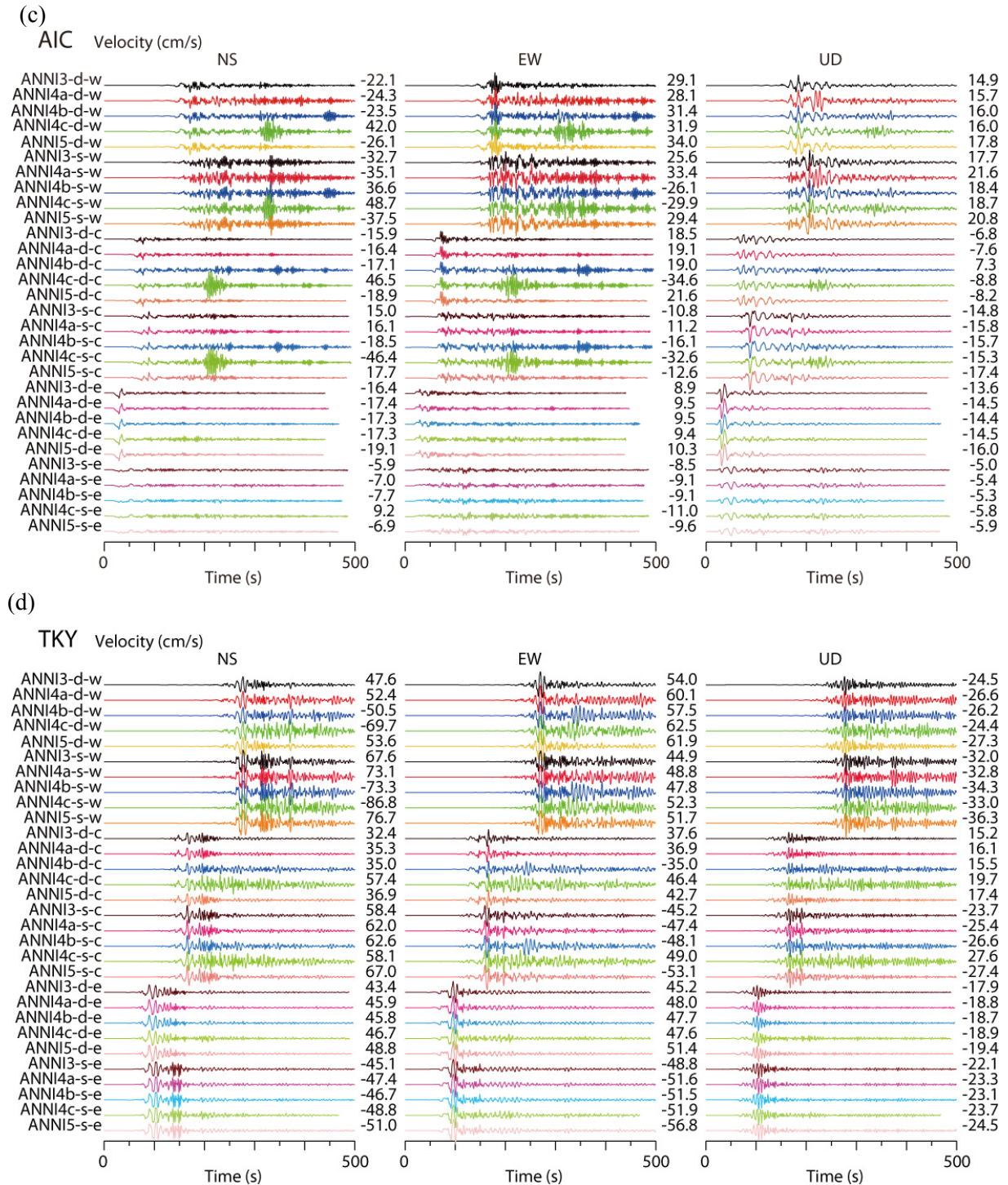


Figure 4.1 continued

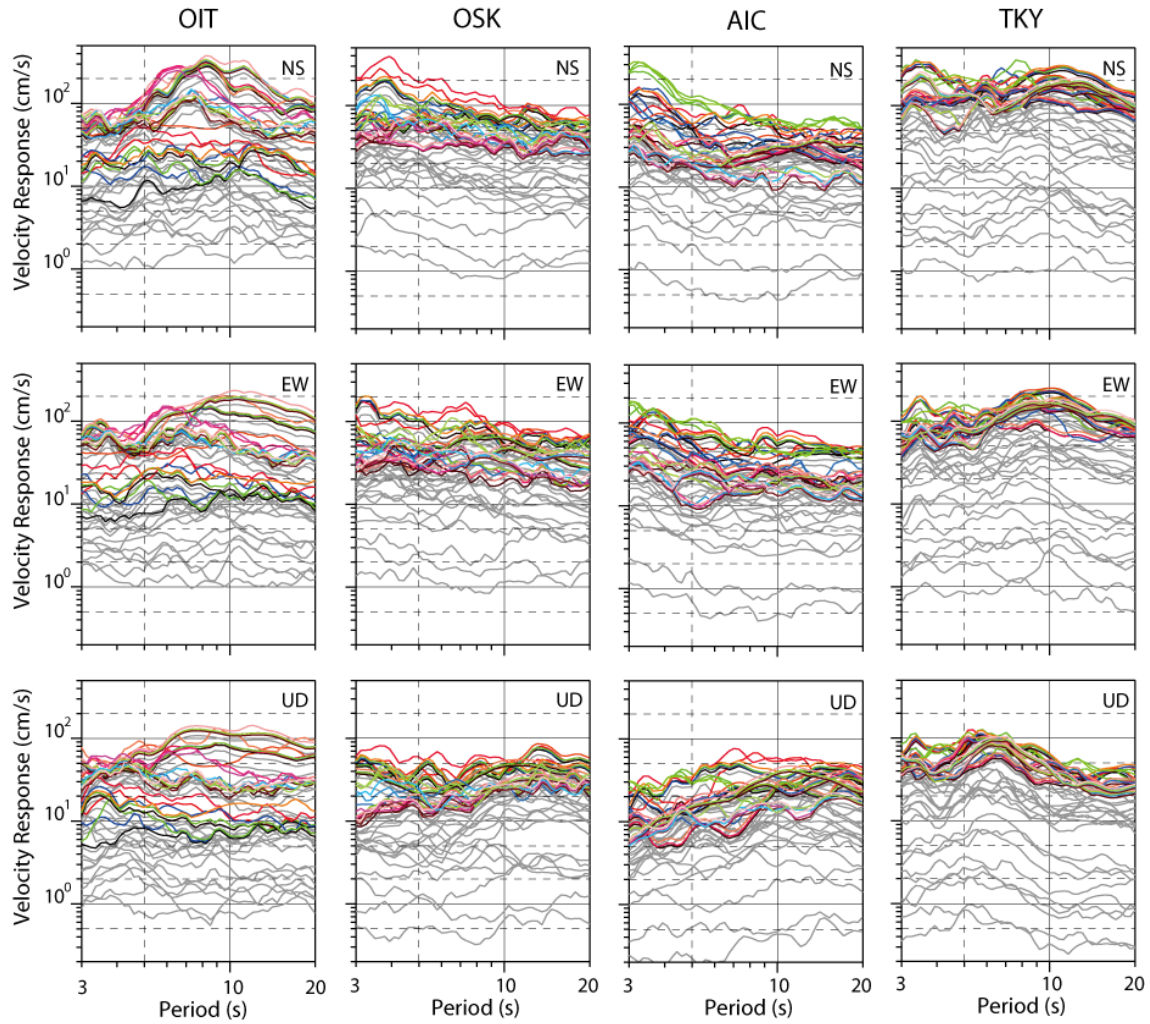


Figure 4.2. Velocity response spectra ($h=0.05$) of the 3-D FD simulation results for 55 scenarios at OIT, OSK, AIC and TKY. Coloured lines correspond to scenarios shown in Fig. 4.1. Grey lines correspond to other smaller scenarios.

AIC and those from the along trough ‘b’ and ‘c’ areas elongate a duration of long-period ground motion at TKY.

Figure 4.2 compares the simulated velocity response spectra for all simulated scenarios. These spectra have large scattering by a factor of few hundred. The spectra of scenarios ANNI3, ANNI4a-c, and ANNI5 at OIT have scattering by a factor of 20, at OSK and AIC by 4~10, and at TKY by 2~4. The scattering at TKY is small because TKY locates on the forward rupture direction of the Tokai area in the scenarios. While, the scattering at OIT is large, because long-period ground motion at OIT depends on whether or not the scenarios include the Hyuga-nada area. Because the difference of seismic moment between the scenarios ANNI3, ANNI4a-c, and ANNI5 is small by a factor of two (Table 2.1), the large scattering indicates the hypocenter and asperity location have greater effect on simulation results than the rupture area.

5. DISCUSSION AND CONCLUSION

Figure 5.1 shows histograms and cumulative frequency distribution of simulated peak ground velocity (PGV) and velocity response spectra (S_v) at period of 5 and 10 seconds. The histograms show contribution of the rupture area. The scenarios with wider rupture areas (colored bars) have larger PGV and S_v than those with smaller rupture areas (grey bars). In particular, the scenarios ANNI4a and

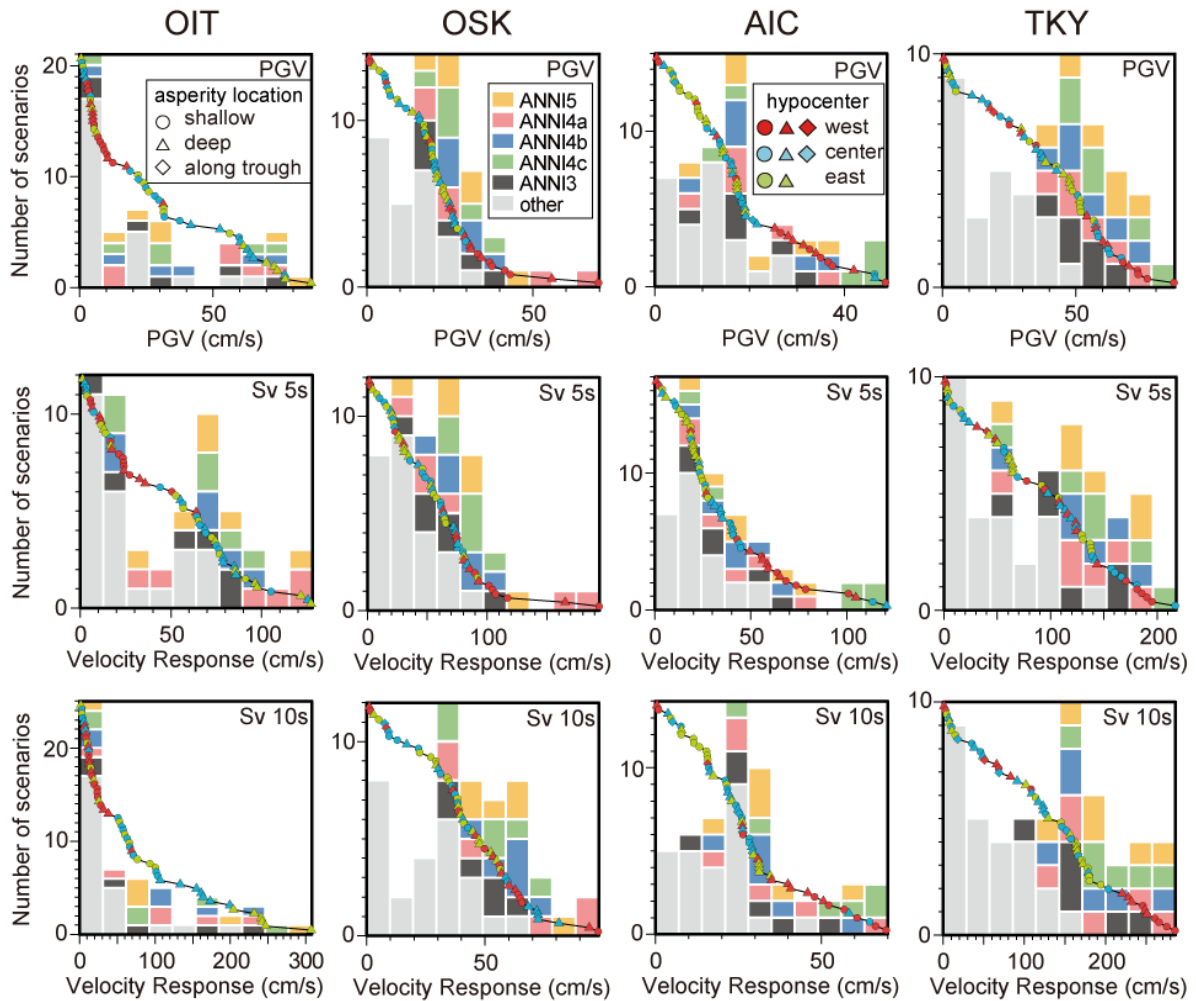


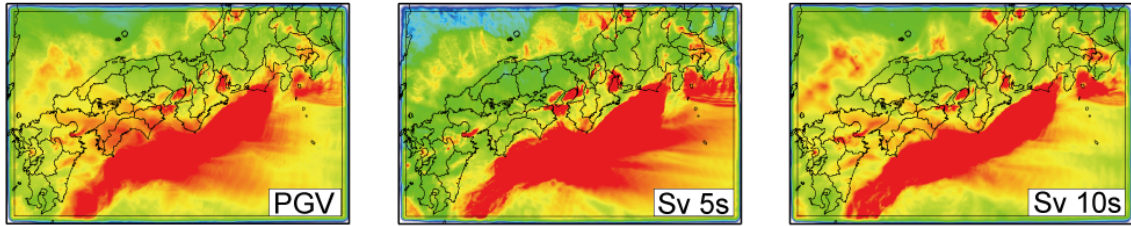
Figure 5.1. Histograms and cumulative frequency distribution of peak ground velocity (PGV) and velocity response spectra (Sv) at period of 5 and 10 seconds for 55 scenarios at OIT, OSK, AIC and TKY. Histograms are colour-coded according to the source area (see PGV panel of OSK). Cumulative curves are colour-coded according to the hypocenter (see PGV panel of AIC) and depicted using different symbols according to the asperity location (see PGV panel of OIT).

ANNI4c generate significantly large PGV and Sv at OSK and AIC, respectively. The cumulative frequency distributions show contribution of hypocenter and asperity location. The scenarios with western hypocenter (red symbols) generate large PGV and Sv at OSK, AIC and TKY, and small PGV and Sv at OIT. The scenarios with deeper asperity (triangles) dominate large PGV and Sv at OIT.

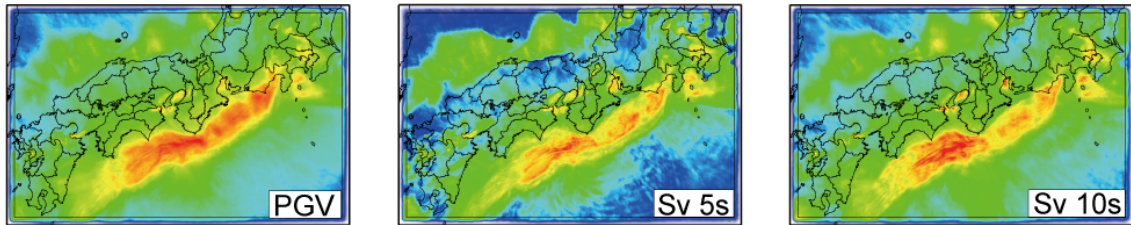
To assess a character of PGV and Sv distribution (Fig. 5.1), we make PGV and Sv maps showing maximum, median (second quartile), interquartile range (iqr: the difference between the third and first quartiles), and maximum scenario using simulation results of 55 scenarios (Figure 5.2). These maps show a possible range of long-period ground motions from the Nankai Trough earthquakes. Large maximum and median values on sedimentary wedge suggest that the sedimentary wedge greatly contributes to the generation of long-period ground motions. The maximum scenario maps show that the scenarios ANNI5 with deep asperity contribute maximum values in the left half area, especially in PGV and Sv 10s. These are the effect of long-period S wave from the Nankai area. In the maximum scenario maps of Sv 5s, the red and green areas distribute in land area wider than PGV and Sv 10s indicating greater effect of the along trough area on Sv 5s values.

In the maximum value maps, the Sv 5s values are larger than Sv 10s values at the Osaka and Nobi basins, while the Sv 10s values are larger than Sv 5s values at the Kanto basin. The Osaka and Nobi basins have large difference between the maximum and median values and have small iqr. This feature

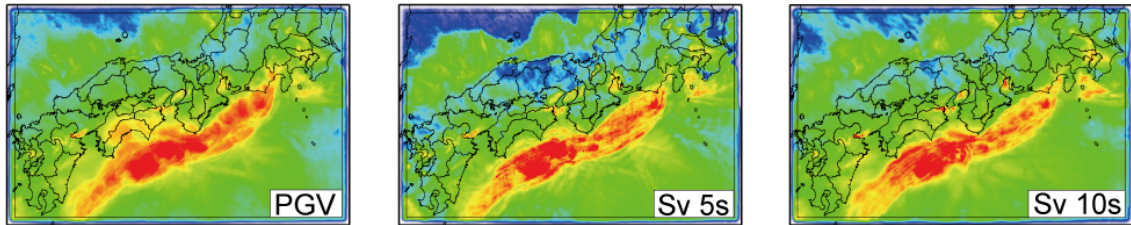
(a) Maximum



(b) Median



(c) Interquartile range



(d) Maximum scenario

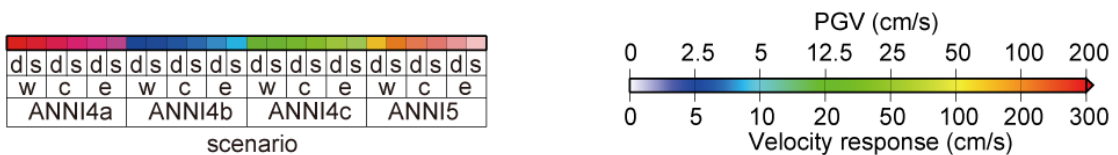
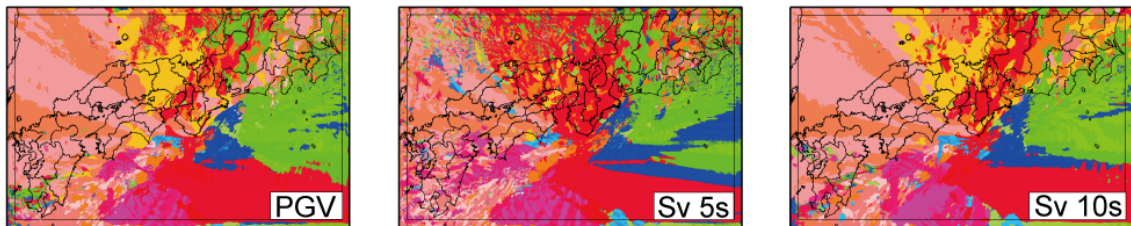


Figure 5.2. Peak ground velocity (PGV) and velocity response spectra (Sv) maps showing (a) maximum value, (b) median value, (c) interquartile range and (d) maximum scenario among 55 scenarios. Colour scales for PGV and Sv are shown in bottom right, and that for the maximum scenario is shown in bottom left.

indicates that these basins are greatly influenced by a few specific scenarios as shown in Fig. 5.1. However, the Kanto basin has relatively large median values and iqr. This indicates that the long-period ground motions in Kanto basin are generally large among the simulated scenarios.

In the FD simulation, we use a Kostrov-like slip velocity time function proposed by Nakamura and Miyatake (2000). However, applying this function to the interplate earthquakes is a contentious issue, especially in a shallow source area. To assess a contribution of source time function, we apply a boxcar like time function to the along trough area. The simulation result shows that PGV values decrease by a factor of two. This indicates that the significant large amplitudes at OSK and AIC as shown in Fig. 5.1 are controlled by selection of the slip velocity function. Selection of appropriate source time function is a future task.

Since the characterized source model does not include short-wavelength heterogeneity, the FD simulation underestimates shorter period components than the dominant period correspond to the asperity size. Considering the large asperities of our source models, the simulation results of this study are affected by this underestimation. We would introduce some kind of heterogeneity into the characterized source model (e.g., Hisada, 2001; Sekiguchi et al., 2008) so that FD simulation appropriately evaluate long-period ground motions. This is also a future task.

ACKNOWLEDGEMENT

Some of the figures in this paper were made using GMT (Wessel and Smith, 1995). This study is supported by the Support Program for Long-Period Ground Motion Hazard Maps of MEXT.

REFERENCES

- Aoi, S. and Fujiwara, H. (1999). 3-D finite difference method using discontinuous grids. *Bulletin of the Seismological Society of America*. **89**, 918-930.
- Aoi, S., Hayakawa, T. and Fujiwara, H. (2004). Ground motion simulator: GMS. *Butsuri Tansa*. **57**, 651-666 (in Japanese with English abstract).
- Earthquake Research Committee (2001). On the long-term evaluation of earthquakes in the Nankai trough. http://www.jishin.go.jp/main/chousa/01sep_nankai/index.htm.
- Furumura, T., Imai, K. and Maeda, T. (2011). A revised tsunami source model for the 1707 Hiei earthquake and simulation of tsunami inundation of Ryujin Lake, Kyushu, Japan. *Journal of Geophysical Research*. **116**, B02308, doi:10.1029/2010JB007918.
- Graves, R. W. (1996). Simulating seismic wave propagation in 3D elastic media using staggered grid finite differences. *Bulletin of the Seismological Society of America*. **86**, 1091-1106.
- Hisada, Y. (2001). A theoretical omega-square model considering the spatial variation in slip and rupture velocity. Part 2: Case for a two-dimensional source model. *Bulletin of the Seismological Society of America*. **91**, 651-666.
- Irikura, K. and Miyake, H. (2001). Prediction of strong ground motions for scenario earthquakes. *Journal of Geography*. **110**, 849-875 (in Japanese with English abstract).
- Koketsu, K., Miyake, H., Fujiwara, H. and Hashimoto, T. (2008). Progress towards a Japan integrated velocity structure model and long-period ground motion hazard map. *Proceedings of the 14th World Conference on Earthquake Engineering*. S10-038.
- Murotani, S., Miyake, H. and Koketsu, K. (2008). Scaling of characterized slip models for plate-boundary earthquakes. *Earth, Planets and Space*. **60**, 987-991.
- Nakamura, H. and Miyatake, T. (2000). An approximate expression of slip velocity time functions for simulation of near-field strong ground motion. *Zisin*. **53**, 1-9 (in Japanese with English abstract).
- Sekiguchi, H., Yoshimi, M., Horikawa, H., Yoshida, K., Kunimatsu, S. and Satake, K. (2008). Prediction of ground motion in the Osaka sedimentary basin associated with the hypothetical Nankai earthquake. *Journal of Seismology*. **12**, 185-195.
- Wessel, P. and Smith, W. H. F. (1995). New version of the Generic Mapping Tools released, *Eos Transactions, American Geophysical Union*. **76**, 329.